

WD-A137 993

GEODETTIC USE OF GEOSAT-R(U) MATHEMATICAL GEOSCIENCES
INC LEXINGTON MA E M GAPOSCHKIN AUG 83 AFGL-TR-83-0254
F19628-82-C-0144

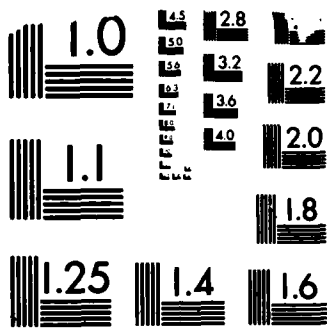
1/1

UNCLASSIFIED

F/G 8/5

NL

END
11-80
G-
770



MICROCOPY RESOLUTION TEST CHART
NATIONAL BUREAU OF STANDARDS-1963-A

AFGL-TR-83-0254

GEODETIC USE OF GEOSAT-A

E. M. Gaposchkin

Mathematical Geosciences Inc.
55 Farmcrest Avenue
Lexington, Massachusetts 02173

Final Report
16 Sept 1982 - 30 Aug 1983

August 1983

Approved for public release; distribution unlimited

AIR FORCE GEOPHYSICS LABORATORY
AIR FORCE SYSTEMS COMMAND
UNITED STATES AIR FORCE
HANSOM AFB, MASSACHUSETTS 01731

DTIC
ELECTE
FEB 15 1984
S D
E

84 02 15 034

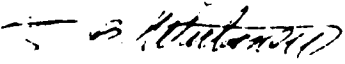
AD A 1 3 7 9 9 3

DTIC FILE COPY

CONTRACTOR REPORTS

This report has been reviewed by the ESD Public Affairs Office (PA) and is releasable to the National Technical Information Service (NTIS).

This technical report has been reviewed and is approved for publication.

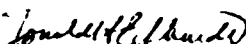


THEODORE E. WIRTANEN
Contract Manager



THEODORE E. WIRTANEN
Acting Chief, Geodesy & Gravity Branch

FOR THE COMMANDER



DONALD H. ECKHARDT
Director
Earth Sciences Division

Qualified requestors may obtain additional copies from the Defense Technical Information Center. All others should apply to the National Technical Information Service.

If your address has changed, or if you wish to be removed from the mailing list, or if the addressee is no longer employed by your organization, please notify AFGL/DAA, Hanscom AFB, MA 01731. This will assist us in maintaining a current mailing list.

Do not return copies of this report unless contractual obligations or notices on a specific document requires that it be returned.

Unclassified

SECURITY CLASSIFICATION OF THIS PAGE (When Data Entered)

REPORT DOCUMENTATION PAGE		READ INSTRUCTIONS BEFORE COMPLETING FORM
1. REPORT NUMBER AFGL-TR-83-0254	2. GOVT ACCESSION NO.	3. RECIPIENT'S CATALOG NUMBER
4. TITLE (and Subtitle) GEODETIC USE OF GEOSAT-A		5. TYPE OF REPORT & PERIOD COVERED Final Report 16 Sept 1982-30 Aug 1983
		6. PERFORMING ORG. REPORT NUMBER
7. AUTHOR(s) E.M. Gaposchkin		8. CONTRACT OR GRANT NUMBER(s) F19628-82-C-0144
9. PERFORMING ORGANIZATION NAME AND ADDRESS Mathematical Geosciences Inc. 55 Farmcrest Ave. Lexington, Massachusetts 02173		10. PROGRAM ELEMENT, PROJECT, TASK AREA & WORK UNIT NUMBERS 3201DMAD
11. CONTROLLING OFFICE NAME AND ADDRESS Air Force Geophysics Laboratory Hanscom AFB, Massachusetts 01731 Monitor/T.Wirtanen/LWG		12. REPORT DATE August 1983
		13. NUMBER OF PAGES 68
14. MONITORING AGENCY NAME & ADDRESS (if different from Controlling Office)		15. SECURITY CLASS. (of this report) Unclassified
		15a. DECLASSIFICATION/DOWNGRADING SCHEDULE
16. DISTRIBUTION STATEMENT (of this Report) Approved for public release; distribution unlimited		
17. DISTRIBUTION STATEMENT (of the abstract entered in Block 20, if different from Report)		
18. SUPPLEMENTARY NOTES		
19. KEY WORDS (Continue on reverse side if necessary and identify by block number) Geodesy, Geoid, Sea Surface Topography, Satellite Altimetry, Geosat-A, Molodensky Integral, Meso Scale, Eddy Field, Troposphere Correction		
20. ABSTRACT (Continue on reverse side if necessary and identify by block number) The Molodensky Integral can be used to compute gravity anomalies from the geoid height. There are two error sources. The error due to limiting the integral to a spherical cap can, in practice, be reduced by using a low degree and order reference field. For example, with a 6 degree radius cap and a 12th degree and order reference geopotential this error is one milligal. The error due to the geoid height error depends on the gravity anomaly block size and variance of the geoid height error. In this case,		

DD FORM 1 JAN 73 1473

EDITION OF 1 NOV 65 IS OBSOLETE

Unclassified

SECURITY CLASSIFICATION OF THIS PAGE (When Data Entered)

a 3 cm rms geoid error will result in a one milligal error for a 28km x 28 km mean gravity anomaly. Quantization error of replacing the integral by a summation and the singularity of the Molodensky Kernel are found to contribute insignificant errors.

The correction for satellite to sea surface altitude measurements due to the wet troposphere (hw) is investigated using Scanning Multichannel Microwave Radiometer (SMMR) data from SEASAT-1. It is found that the total variance of hw is (22.5)**2. This is dominated by a mean latitude dependent variation. The variance with respect to this mean is (4.5cm)**2 with a correlation 0.28 at a distance of 43 km (the SMMR resolution). Using a climatological means will allow this correction to be made with 5cm accuracy. If meteorological data from weather hindcasts, e.g., from the Fleet Numerical Oceanographic Center (FNOC), are used, hw can be predicted with an accuracy of (3.9cm)**2. The mean FNOC generated correction differs from the mean SMMR correction by 0.01cm. The variance of the FNOC generated correction with respect to the mean is (2.3cm)**2. Therefore, the FNOC data is suitable for determination of the climatological means. Finally, by averaging as few as 15 measurements, the error due to uncertainty in hw can be decreased. The improvement does not continue as \sqrt{n} but seems to asymptotically approach (2cm)**2.

The Mesoscale Eddy field is discussed, and is shown to contribute 8 to 25 cm rms noise to the mean sea surface.

Accession For	
NTIS GRA&I	<input checked="" type="checkbox"/>
DTIC TAB	<input type="checkbox"/>
Unannounced	<input type="checkbox"/>
Justification	
By _____	
Distribution/	
Availability Codes	
Dist	Avail and/or Special



TABLE OF CONTENTS

		<u>Page</u>
	ABSTRACT	
I.	INTRODUCTION.....	1
II.	ESTIMATE OF ACCURACY N -- Δg	4
III.	MODIFIED MOLODENSKY INTEGRAL AND ITS ACCURACY...	7
IV.	AN ALGORITHM FOR THE MOLODENSKY INTEGRAL	14
V.	COMPUTATION OF THE INNER ZONE.....	17
	1) Spline Fit.....	17
	2) Least Squares Fit.....	18
VI.	SUMMARY OF MOLODENSKY INTEGRAL.....	22
VII.	INSTRUMENT AND ORBIT ERROR.....	24
VIII.	THE OCEANOGRAPHIC FIELD.....	27
	1) Mean Circulation.....	27
	2) Eddy Field.....	27
IX.	ENVIRONMENTAL CORRECTIONS, A SURVEY.....	32
X.	TROPOSPHERIC REFRACTION.....	34
	1) Basic Principles.....	34
	2) The Seasat SMMR Data Analyzed.....	37
	3) The Regional Variation of Wet Troposphere Correction.....	38
	4) Spectra of Wet Troposphere Correction.....	43
	5) Discussion of Wet Troposphere Error.....	50

TABLE OF CONTENTS (cont.)

	<u>Page</u>
XI. SUMMARY.....	52
XII. ACKNOWLEDGEMENTS.....	56
XIII. REFERENCES.....	57
APPENDIX A: ERROR FUNCTION.....	60

I.

INTRODUCTION

Satellite to sea surface altimeter data can be used to estimate surface gravity (Δg) in ocean areas by assuming the mean sea surface (ζ) measured with the altimeter, suitably corrected, is the geoid (N). The Geos-3 and Seasat-1 radar altimeters have demonstrated the concept and Geosat-A will, hopefully, provide systematic and complete coverage of the world's oceans. We will discuss the procedures and errors to be expected with Geosat-A in three broad categories.

1. Measurement of Sea Surface
 - (a) Accuracy of the altimeter
 - (b) Accuracy of Geosat-A ephemeris
2. Non-geodetic contributions to observed sea surface
 - (a) Oceanographic signals
 - (b) Environmental corrections
3. Integral for calculations of Δg from N
 - (a) Integration limited to a spherical cap
 - (b) Error propagation

In general these are all complex issues. In particular 2.a and 2.b involve much of what is known as physical oceanography and tropical meteorology. We will narrow the discussion by focusing on a particular objective and data analysis strategy; viz. calculation of Δg in the world's oceans. One can describe this as follows. The end product is a global map of gravity at sea with a resolution of, say, 15 minutes (15'). This gravity map will be determined from a geoid surface obtained from combining data, taken over more than 10 years, from Geos-3, Seasat-1, and Geosat-A. The compu-

tation will be made with a Molodensky type integral using data within a spherical cap of a few degrees. The computation will use a reference surface, say WGS83, truncated at some degree and order, and aim for an accuracy of a milligal or better.

The accuracy of recovered gravity anomalies depends on the accuracy of the geoid and the resolution sought as illustrated in Table 1. Table 1 illustrates the relation between geoid and gravity accuracy for a number of block dimensions a and b . Since the relation scales it can be used for any assumed accuracy. For example, for a 10km x 10km square, a geoid uncertainty of $M=1\text{cm}$ would produce a gravity anomaly map of $n=0.76\text{ mgal}$.

The mathematical relation to calculate a gravity anomaly (Δg) from geoid height (N) is a (singular) integral equation due to Molodensky (Molodensky, et al., 1962). The error in this estimate has two sources: First, observation errors (e) and real physical departures of the geoid (N) from the mean sea surface (ζ), and second, errors in the numerical implementation of the integral. The first error source is due to, for example, satellite orbit error, ocean currents, tides, storm surges, salinity and temperature variations, and eddies. In general these vary with time and position, and have a maximum amplitude of about one meter. The large amplitudes have time variability of weeks to months, and with data taken for several years, they may average out. These 'errors' will be discussed in this Report.

The second error source has two parts. The first is due to the fact that the area of integration for the Molodensky integral is the whole unit sphere. In other words this calculation assumes complete coverage of the geoid. Forming the complete integral is impractical. In addition, the

altimeter only provides geoid data in the oceans. Therefore, the integration is limited to a spherical cap around the integration point. The error due to neglecting this outer zone can be quantified. Secondly, the integral must in practice be replaced by a finite summation. This error of quantization must also be considered. However, the integration error from limiting the area of integration to a spherical cap can be made less than a milligal by use of a suitable reference geoid and spherical cap size (Sections II, IV, V, and VI; Gaposchkin, 1983). We proceed to analyze the Molodensky integral, and examine an implementation of this integral.

II.

ESTIMATE OF ACCURACY $N \rightarrow dg$

We begin by finding a general relation between the accuracy of mean gravity anomalies (Δg) and mean geoid heights (N) for areas with sides a and b assuming complete knowledge of N or Δg . Following Moritz (1974) we start with Stokes' formula:

$$N = \frac{R}{4\pi\gamma} \int_{\sigma} S(\psi) \Delta g \, d\sigma \quad (1)$$

where R is the earth's mean radius, γ is the mean value of gravity, $S(\psi)$ is the Stokes function, and σ is the unit sphere. We set by error propagation:

$$M^2 = \frac{L}{8\pi\gamma^2} \int_0^{\pi} [S(\psi)]^2 \sin\psi \, d\psi \quad (2)$$

where M is the standard error of the geoid height (N). It is shown (Moritz, 1974) that for square blocks of side a , with $L = a^2 \, \text{m}^2$,

$$M^2 = \frac{a^2 \, \text{m}^2}{4\pi\gamma^2} \Psi(n_0) \quad (3)$$

where M is the standard error of the gravity anomaly (Δg), and

$$\Psi(n_0) = \sum_{n=2}^{n_0} \frac{2n+1}{(n-1)^2} \quad (4)$$

and

$$n_0 = \frac{\pi R}{a} \quad (5)$$

We generalize (3) and (5) for rectangular block of sides a and b as:

$$M^2 = \frac{a b m^2}{4 \pi \gamma^2} \psi(n_0) \quad (6)$$

$$n_0 = \frac{\pi R}{\sqrt{ab}} \quad (7)$$

The function $\psi(n_0)$ is very slowly changing and in our range of interest is approximately 20. Equation (6) can be used to estimate the gravity accuracy given a geoid accuracy, or to estimate a geoid accuracy given a gravity accuracy. Table 1 lists values for various M, m, a, and b.

TABLE 1
 UNCERTAINTY FOR GRAVITY ANOMALY VS. GEOID HEIGHT

<u>a</u> (Km)	<u>b</u> (Km)	<u>n_o</u>	<u>ψ (n_o)</u>	<u>M</u> (cm)	<u>m</u> (mgal)
1	1	20000	25.173	10	69.94
10	10	2003	21.292	13	10.0
10	10	2003	21.292	10	7.6
25	12.5	1133	20.151	10	4.55
20	20	1001	19.903	26	10.0
20	20	1001	19.903	10	3.93
25	25	801	19.456	31	10.0
25	25	801	19.456	10	3.18
50	50	401	18.067	61	10.0
50	50	401	18.067	10	1.65
100	100	200	16.665	118	10.0
100	100	200	16.665	10	0.86

For example, a 15'x15' grid at a latitude of 60 degrees would be a rectangle of approximately 28km x 18km. Ten cm geoid heights would correspond to 4.55 milligal gravity anomalies. Since these variances scale, 1 cm geoid heights would correspond to 0.455 mgal gravity anomalies, and 25cm geoid heights would correspond to 11.4 mgal gravity anomalies. These estimates are confirmed very well in the simulations using the Molodensky integral.

III.

MODIFIED MOLODENSKY INTEGRAL AND ITS ACCURACY

The Molodensky integral (Molodensky, et al., 1962) is generally written as:

$$\Delta g_p = - \frac{\gamma N_p}{R} - \frac{\gamma}{2\pi} \int_{\sigma} \frac{N - N_p}{r_p^3} d\sigma \quad (8)$$

where Δg_p and N_p are the gravity anomaly and geoid height at the computation point p and r_p is the cord distance between the point p and the differential area element $d\sigma$. Now:

$$r_p = 2R \sin(\psi/2) \quad (9)$$

where ψ is the central angle between point p and the area element $d\sigma$, and:

$$d\sigma = R^2 \sin\psi \, d\psi \, d\alpha$$

The Molodensky integral is a global integral and in principle requires knowledge of N everywhere. In addition, in practice the integral (8) is replaced with finite sums. Also, as a practical matter N is not known everywhere and considerable simplification and economy is achieved by limiting the summation to geographical regions near the computation point p . The quantization error is explored here with a numerical simulation.

The effects of neglected zones outside a spherical cap has been investigated by Buglia (1976). Buglia proceeded to write the integral (8) in two parts: one for the integral within a spherical cap of angular radius ψ_0 , and a second part for the remaining area of the unit sphere, which we call the outer zone (Buglia, 1976, eq 3). He calls the second integral E_p , the "error of commission". He then found an expression for E_p , to be used for estimation of the error of the mean global error. In summary we have:

$$\Delta g_p = -\frac{\gamma N_p}{R} - \frac{\gamma}{16\pi R} \int_{\psi=0}^{\psi_0} \int_{\alpha=0}^{2\pi} f(\psi) (N-N_p) \sin\psi d\psi d\alpha - E_p \quad (10)$$

and

$$f(\psi) = \frac{1}{\sin^3(\psi/2)} \quad (11)$$

Now we can expand N in a series of surface harmonics of degree n , as:

$$N = \sum_{n=2}^{\infty} N_n = \sum_{n=2}^{\infty} N_n (\phi, \lambda) = \sum_{n=2}^{\infty} N_n (\psi, \alpha) \quad (12)$$

and

$$E_p = \frac{\gamma}{8R} \left(R_0 N_p - \sum_{n=2}^{\infty} R_n N_n \right) \quad (13)$$

where

$$R_0 = 4 \frac{1 - \sin(\psi_0/2)}{\sin(\psi_0/2)}, \quad R_1 = R_0 - 8 [1 - \sin(\psi_0/2)] \quad (14)$$

$$R_n = \frac{2 [P_{n-2}(\cos \psi_0) - P_n(\cos \psi_0)]}{(n-1) \sin(\psi_0/2)} + 2 R_{n-1} - R_{n-2}$$

and $P_n(x)$ are Conventional Legendre Polynomials. Buglia (1976) gives tables of R_n , recalculated here in Appendix A.

Now equation 10 is an identity. That is, if all the N_i were known, we assume N_p is known, then E_p could be calculated, subtracted from the integral over the cap, and Δg_p would be known without any error from neglecting the outer zone. Of course the N_i are not completely known, or we would not need to continue this exercise. Even so, we can calculate the $R_0 N_p$ part of E_p . In addition we note that if some of the N_n are known, their contribution to E_p can be computed. We could assume the lower degree coefficients of the geopotential are known with sufficient accuracy to adopt them as known. In this case the simplest procedure is to subtract this known geopotential surface of degree and order n_0 from the

geoid height data and we have:

$$E_p = \frac{\gamma}{gR} \left(R_0 N_p - \sum_{n=n_0+1}^{\infty} R_n N_n \right) \quad (13)$$

to calculate the error in neglecting the outer zone.

Finally one can profit from the variation of R_n and N_n with increasing n . Recall that we can write:

$$N_p = \sum_{n=2}^{\infty} N_n (\alpha = 0, \psi = 0) \quad (15)$$

and note that

$$\sum_{n=n_0+1}^{\infty} R_n N_n (\alpha = 0, \psi = 0)$$

is a linear combination of the N_n . For example, if we assume that present geopotential models are sufficiently accurate to degree 10, and we elect to use a spherical cap with $\psi_0=5^\circ$, then the relevant values of R_n , $n=11, 12, \dots$ decrease slowly from 22.26617 to 0.029020 at degree 18. However, we don't, in general, know N_n for each computation point.

Now, in general, if we assume a geopotential model is sufficiently well known through degree and order n_0 , i.e., the unknown harmonics are of degree n_0+1 and higher, we can write:

$$\begin{aligned}
 E_p &= \frac{\gamma}{8R} \left(R_0 N_p - R_{n_0+1} N_p - \sum_{n=n_0+1}^{\infty} (R_n - R_{n_0+1}) N_n \right) \\
 &= \frac{\gamma}{8R} \left(R_0 - R_{n_0+1} \right) N_p - E_p^* \quad (16)
 \end{aligned}$$

$$E_p^* = \frac{\gamma}{8R} \sum_{n=n_0+2}^{\infty} (R_n - R_{n_0+1}) N_n \quad (17)$$

where we can compute the first part of 16, and the remaining error E_p^* is smaller than E_p . Therefore the actual Molodensky integral should be written:

$$\Delta g_p = - \frac{\gamma}{R} \left[1 - \frac{R_0 - R_{n_0}}{8} \right] N_p - \frac{\gamma}{16\pi R} \int_{\psi=0}^{\psi_0} \int_{\alpha=0}^{2\pi} f(\psi) (N - N_p) \sin \psi d\psi d\alpha \quad (18)$$

which we call the Modified Molodensky Integral.

We can now establish the global mean square error for E_p^* as:

$$M \left\{ E_p^{*2} \right\} = \frac{\gamma^2}{64 R^2} \sum_{n=n_0+2}^{\infty} (R_n - R_{n_0})^2 M \left\{ N_n^2 \right\} \quad (19)$$

Using the celebrated $10^{-5}/n^2$ rule for the anomalous potential we have:

$$M \left\{ N_n^2 \right\} = R^2 \times 10^{-10} (2n+1)/n^4 \quad (20)$$

$$M \left\{ E_p^{*2} \right\} = \frac{\gamma^2 \times 10^{-10}}{64} \sum_{n=n_0+2}^{\infty} (R_n - R_{n_0})^2 \frac{(2n+1)}{n^4} \quad (21)$$

Table 2 shows representative values for this error term.

The case $n_0=0$ is adopting no reference geopotential model. For practical limitations of a spherical cap radius of 20° or less, the error of omitting the outer zone exceeds several hundred milligals.

It is customary to assume that the reference ellipsoid is correctly positioned with respect to the earth's center of mass and principal moments of inertia. In this case, one actually assumes knowledge of the reference surface $n_0=2$, and the Modified Molodensky Integral provides an accuracy of several tens of milligals. In fact there would be terms of degree and order 2 remaining, and a more careful calculation should be made for the case of adopting a best fitting ellipsoid in contrast to a reference surface of degree two.

However, adopting a reference geopotential of degree and order 12, and using a spherical cap of 6° would give a 1.24 milligal gravity anomaly. Table 2 can be used as a prescription for choosing the cap size and reference geopotential model for any desired gravity anomaly accuracy, due to neglecting the outer zone in the integral. It also dramatically illustrates the benefits of using an accurate low degree and order reference geopotential model. With an accurate geopotential model of degree and order 18 and a six degree integration cap, the error due to ignoring the outer zone would be reduced to 0.07 milligals.

TABLE 2
MODIFIED MOLODENSKY FORMULA ERROR (MGALS)

ψ_0	m_0	0	2	4	6	8	10	12	14	16	18
4		462.80	151.07	73.85	40.37	23.05	13.35	7.71	4.39	2.44	1.30
5		418.24	121.94	53.66	26.25	13.24	6.65	3.24	1.50	0.64	0.26
6		381.68	99.86	39.49	17.16	7.53	3.18	1.24	0.43	0.14	0.07
7		350.76	82.59	29.27	11.19	4.17	1.42	0.42	0.12	0.07	0.09
8		324.07	68.80	21.77	7.22	2.23	0.58	0.13	0.07	0.10	0.12
9		300.66	57.60	16.19	4.60	1.13	0.22	0.07	0.10	0.12	0.12
10		279.86	48.40	12.01	2.86	0.54	0.09	0.09	0.12	0.12	0.09
11		261.21	40.77	8.87	1.73	0.24	0.07	0.12	0.13	0.09	0.05
12		244.34	34.40	6.50	1.01	0.11	0.09	0.13	0.11	0.06	0.03
13		229.00	29.05	4.72	0.56	0.07	0.12	0.13	0.08	0.03	0.01
14		214.96	24.53	3.39	0.30	0.08	0.13	0.11	0.05	0.02	0.00
15		202.06	20.71	2.40	0.16	0.10	0.13	0.09	0.03	0.01	0.00
16		190.15	17.47	1.67	0.09	0.12	0.12	0.06	0.02	0.00	0.01
17		179.13	14.71	1.14	0.07	0.13	0.11	0.04	0.01	0.00	0.01
18		168.89	12.37	0.76	0.08	0.14	0.08	0.02	0.00	0.01	0.01
19		159.36	10.37	0.49	0.09	0.13	0.06	0.01	0.00	0.01	0.01
20		150.46	8.67	0.31	0.11	0.12	0.04	0.01	0.00	0.01	0.00

IV.

AN ALGORITHM FOR THE MOLODENSKY INTEGRAL

The practical implementation of the Molodensky Integral investigated here is taken from a computer code developed at DMAAC (St. Louis) and kindly provided to MATHEMATICAL GEOSCIENCES INC. for this study.

The Molodensky program assumes a data base exists, with complete coverage of the region of interest. The spherical region is gridded in latitude and longitude, resulting in rectangular areas. The gridding is uniform, and for this purpose was chosen to be 15 minute by 15 minute rectangles. The region selected for study was at approximately 60° latitude. Therefore the areas were approximately 28km x 14km rectangles.

The Molodensky program, takes as input the region containing the computation points, the spacing of the computation points, and the cap size. Then, for each computation point, all the points in the spherical cap are extracted from the data base and the quadrature is performed. The rectangle containing the computation point (called the inner zone) is treated separately, necessitated by the singularity of the Kernel (11) at the computation point. This square is subdivided with a uniform 6x6 grid. A two dimensional bi-cubic spline is fit to the 25 points closest to the computation point. The spline fit is used to calculate the geoid values on the 6x6 grid. These 36 sub areas are then integrated in the same way as the other rectangles. The treatment of the inner zone will be discussed further in Section V. The actual integration takes the value of the Kernel at the center of the rectangle, and multiplies by the area of the region. As will be seen, this quantization works satisfactorily.

This program has been modified in a number of ways. First, for testing purposes, the data base was expanded to include a computed gravity anomaly at each grid point. When developing simulated data for testing, the gravity anomaly was also calculated and included in the data base. The program was modified to retrieve the gravity anomaly and compare the value computed from the Molodensky Integral with the simulated value. Next, the program was modified to calculate and explicitly use the error function (R_n , eq 14) and explicitly use the Modified Molodensky Integral (18). Finally, alternate methods to treat the inner zone were developed (see Section V).

The simulated data base was developed using potential coefficients. In addition, noise was added to the data. The first tests were done to show the whole calculation was self-consistent. For this, recall that the Modified Molodensky Integral has an error term (17) that involved surface harmonics of degrees greater than the reference field employed. For this simulation, only harmonics of degree twelve were used. Therefore, the error term, for higher harmonics, should be exactly zero. The root mean square agreement of gravity anomalies estimated with the Modified Molodensky formula, and the original values was 0.047 mgals. This departure from zero is consistent with the accuracy of the geoid values and gravity anomalies stored in the data base (1 millimeter, and 10 microgals). The same data was corrupted with 10 cm Gaussian Noise. In this case the standard error was 14.958 milligals. The results are summarized in Table 3.

TABLE 3

MODIFIED MOLODENSKY PROGRAM ACCURACY
 REFERENCE FIELD 12TH DEGREE ONLY

sigma on data (cm)	sigma (Δg) (mgal)
< 0.1	0.047
10.0	14.958

The fact that the zero noise case agreed so well demonstrated that the basic theory and implementation work. However, the significant disagreement of the estimate with Table 1 mandates further investigation. In particular the treatment of the inner zone and the geoid value at the computation point have been found to be critical. The original code performed a spline fit to the nearest 25 points to the computation point. It determined 64 spline coefficients, i.e., more unknowns than observations. Therefore the fit was essentially an interpolation exactly matching the observed values, including the computation point. Any error at the computation point directly corrupts every point in the integration since the integration involves $N - N_p$. We therefore explored the treatment of the inner zone, to improve the value N_p and to improve the treatment of the inner zone integral.

V.
COMPUTATION OF THE INNER ZONE

V.1. Use of the Bicubic Spline Fit

As discussed above, the spline fit was made to interpolate the 25 points closest to the computation point. Its primary use is for calculation of N near to N_p on a grid finer than the data are given. The interpolation, in fact, must go through the computation point because the kernel is singular at the computation point. Put another way, near the computation point $N - N_p$ must approach zero faster than $\sin^3(\psi/2)$ or the integration is singular.

The number of data points used for the spline fit was extended from 25 to 81. The calculation then had fewer unknowns than data points, which results in a kind of Least Squares fit to the data. However, the spline still fit exactly at the computation point, and did not allow an improved value of N_p . However, the values of N used in the inner zone improved the fit to 12.198 milligals.

To further quantify the effect of errors in N_p and the inner zone, on the gravity anomaly, the true values of N were used, i.e., noise was not added to the values used for calculating the spline fit and interpolation in the inner zone. Therefore in the integration, the true value of N_p and the inner zone integral were used. In this case the fit was improved to 2.884 milligals. Of course, this could never be achieved in practice, since one never knows the true value of N_p . This shows, however, the absolute necessity for optimum treatment of the geoid values at the computation point.

This demonstration that the inner zone treatment is a primary error source in the quadrature led to alternate methods of treating the inner zone.

V.2. Least Squares Fit for the Inner Zone

The weakness of the spline fit is that it does not provide a Least Squares estimate of the polynomial coefficients, N_p , and N within the inner zone. We therefore sought a fit to a number of values of N near to N_p . We selected the simple relation:

$$N(x, y) = \sum_{i+j \leq 3} a_{ij} x^i y^j + a_{22} x^2 y^2 \quad (23)$$

where x, y are coordinates with respect to the computation point. Therefore:

$$N_p = N(0, 0) = a_{00} \quad (24)$$

This would provide the desired Least Squares estimate of N_p . As a second benefit, we can directly estimate the inner zone integral from the coefficients a_{ij} .

If we assume $d\sigma$ is small, then in the limiting flat earth approximation, the Molodensky Kernel becomes:

$$f(\psi) = \frac{1}{\sin^3(\psi/2)} = \frac{8}{r^3} = \frac{8}{(x^2 + y^2)^{3/2}} \quad (25)$$

Now, consider the integral in (18):

$$I = \int_{\psi=0}^{\psi_0} \int_{\alpha=0}^{2\pi} \frac{N - N_p}{r^3} dA = \int_{\psi=0}^{\psi_0} \int_{\alpha=0}^{2\pi} \frac{N(x,y) - N(0,0)}{r^2} d r d \alpha = \sum A_{ij} \quad (26)$$

The only non zero integrals are:

$$A_{2,0} = A_{0,2} = \pi, \quad A_{22} = \pi/12 \quad (27)$$

So the integral for the inner zone is:

$$\Delta g_{\text{inner}} = - \frac{\gamma}{2R} \left\{ (a_{20} + a_{02}) r_0 - a_{22} r_0^3 / 12 \right\} \quad (28)$$

This relation illustrated the nature of the Molodensky integral. The Stokes Integral (1) to obtain the geoid (N) from gravity anomalies (Δg) is essentially a smoothing operation. One can tell this naively from the fact that a geoid map is much smoother than a gravity map. The inverse process to obtain gravity (Δg) from the geoid (N) must be the inverse, or a roughing operation. Equation (29) shows that the Molodensky Integral essentially uses the second degree curvature of the geoid to infer gravity, i.e., 2nd and higher derivatives. It also points out what we already know, that the absolute value of the geoid doesn't play a role in estimating gravity, only the derivatives. The roughing character of the Molodensky Integral must therefore amplify short wavelength variations in N, which is serious if these short wavelength variations are errors.

With this Least Squares fit for the inner zone, a number of experiments can be performed. First, the fit was used with the noiseless data. In this case, the fit was 0.015 milligals rms. This improvement over the spline fit interpolation, 0.047 mgals, was due to improvement of N_p at the submillimeter level.

To test the analytical integral of the inner zone (28), one can do two things. The inner zone is a rectangle, in fact it is a trapezoid but far from the pole this error is small and is ignored, and (28) is for a circle. One can choose the circle's radius such that it has the same area as the rectangle, i.e.:

$$r_o = \sqrt{\frac{ab}{\pi}}$$

Alternatively one can choose $r_o = b$, the smaller dimension, and integrate the remaining area of the rectangle as before. In this case one selects areas in the inner zone to include in the integral, those areas with a mid point outside the radius r_o . There is an error associated with either approach. In both cases more careful calculation could be developed, but this doesn't seem worth pursuing given the quality of the fit. In both cases the fit to the noiseless data was 0.018 milligals, verifying the analytical integral. This small difference between the direct numerical quadrature of the 6x6 inner zone grid and the analytical formula is also true for treating data with Gaussian Noise. Therefore we adopted the direct numerical quadrature for actual calculation.

Finally, the Least Squares polynomial fit was used to obtain gravity anomalies from data with 10cm Gaussian noise. The rms came to 5.033

milligals, which is in satisfactory agreement with 4.55 milligals from Table 1. The results of all these numerical experiments are summarized in Table 4.

TABLE 4
ACCURACY OF MODIFIED MOLODENSKY INTEGRAL
REFERENCE FIELD DEGREE 12 ONLY

<u>Inner Zone</u>	<u>Noise on Data (cm)</u>	<u>Sigma (Δg) (mgal)</u>
Spline to 25 points	< 0.1	0.047
Spline to 25 points	10.0	14.958
Spline to 81 points	10.0	12.198
Spline to 81 points (no inner zone noise)	10.0	2.884
Least Squares Polynomial	< 0.1	0.015
Least Squares Polynomial (Analytical Inner Zone)	< 0.1	0.018
Least Squares Polynomial	10.0	5.033

VI.

SUMMARY OF MOLODENSKY INTEGRAL

The numerical calculation of gravity anomalies from geoid data (as obtained for example, from satellite to sea surface altimetry) has been discussed in terms of the Molodensky Integral. Four sources of error have been investigated:

- 1) Error from the neglected outer zone
- 2) Error from singularity of Molodensky Kernel
- 3) Error from Quantization due to replacing an integral with a summation
- 4) Error from Gaussian noise on the data.

It is found that error 2) and 3) are negligible.

The use of a spherical cap is imposed in two ways. First, as a practical matter performing a quadrature over the whole unit sphere is prohibitive, and second, with a satellite to sea surface altimeter, one does not have geoid data everywhere. A Modified Molodensky Integral (18) is given that reduces the error in neglecting the outer zone. Further significant improvements can be made by using a reference geopotential model for the low degree and order harmonics. Table 3 gives the expected errors in gravity anomalies for a given spherical cap size and reference geopotential models. Today geopotential models are quite accurate to degree and order 10, and significant improvements may be available in the next five years. The benefits in using a reference geopotential model are enormous.

Numerical experiments using simulated noisy data, confirm the a priori accuracy assessments, Table 1. For example, with 10cm geoid values a 15'x15' gravity anomaly can be obtained with an accuracy of approximately

5 milligals. To obtain this accuracy it is essential to treat the geoid at the computation point carefully. This leads to the second conclusion that special care must be taken to achieve the most accurate geoid values. In particular to reach one milligal for 15'x15' areas one must have two cm geoid values.

The implications for processing the Seasat-1 and Geosat-A data are clear. Great care must be taken for all error sources. The long wavelength orbit errors are not critical as long as the orbit bias has been removed with a crossing arc analysis or an orbit matching adjustment such as the spline fit used by Cloutier et al (1981). However, any such fit must be achieved with centimeter accuracy. In addition, parasitic errors such as refraction, real oceanographic signals, and instrument noise must be eliminated to the extent possible. The lack of a radiometer on Geosat-A such as was available on Seasat-1 could create a serious lack of important data. Approaches to these problems will be discussed in the next part of this Report.

VII.
INSTRUMENT AND ORBIT ERROR

The accuracy of the altimeter is fixed. The Geosat-A altimeter is intended to be identical to that on Seasat-1. The characteristics are summarized in Table 5. There are several instrument related corrections necessary. For example, the significant wave height or sea state bias has been analyzed (Born, Richards, & Rosborough, 1982; Hayne & Hancock, 1983; West, 1981). None of these analyses give formal statistics. However, it is estimated that the uncertainty in the sea state bias is 2% of the significant wave height. Therefore for $h_{1/3} < 2.5$ m, one would have less than 5cm rms error. There is also the response of the phase lock loop in the altimeter tracker. In regions of rapid change of altitude, this is an important correction (Tapley, Born, & Parke, 1982).

TABLE 5
ALTIMETER CHARACTERISTICS

<u>Observable</u>	<u>Specification</u>
Altitude (Seasat)	8 cm (precision) $h_{1/3} < 5$ m
Altitude (Geosat*)	3.5 cm (precision)
Significant Wave Height	10% or 0.5m
Swath Width	2.4 to 12 km depends on seastate

*Target for Geosat-A, CDR November 1982.

The absolute accuracy of the Geosat-A ephemeris is beyond the scope of this investigation. There are a number of approaches that can be used to optimize it. Of course, some improvement of the orbit accuracy over that for Seasat-1 will naturally come from two things: 1) Geosat-A is physically more compact, without the large antennae that were on Seasat-1. This will reduce the errors in modelling solar radiation pressure and atmospheric drag. 2) There are improved gravity field models available, some derived using Seasat-1 data, that will also result in more accurate ephemerides.

In addition, methods have been developed to use the observations at altimeter track crossing points to obtain improved estimates of the long wavelength orbit errors. These all use the (erroneous) idea that the sea surface height at each crossing point is a constant. Therefore, any difference in the observed height is assumed to be an error in the radial component of the satellite ephemeris. This would be true if there were no time variable oceanographic, meteorological, and observation biases. Within this assumption, crossing arc analyses have achieved (<10cm), Cheney & Marsh from 1.5 years of Geos-3 data, (15 to 22 cm) Cloutier, and (28 cm) Rapp with Seasat-1 data. One would suppose these to be optimistic estimates since a number of the time variable biases have periods longer than the span of Seasat-1 data, 3 months. Conversely, one would not expect the oceanographic and meteorological errors to be correlated with orbit errors. However, one expects orbit errors to be correlated with geoid errors (Anderle & Hoskin, 1977).

In summary, considerable progress is necessary to reduce the Geosat-A orbit error to the accuracy of the Geosat-A altimeter. For the initial analysis of Geosat-A data, this error source, after the crossing arc analysis has been applied, should be significantly less than 20cm. With

Geosat-A and other data, we can expect the orbital models to approach the instrument accuracy.

VIII.

THE OCEANOGRAPHIC FIELD

VIII.1 The Mean Circulation

The principal non-geodetic signal in the altimeter data comes from the ocean circulation and eddy field. The mean ocean circulation, if it can be defined, would be a position dependent, time invariant signal, and indistinguishable from the geoid with an altimeter. It has an amplitude of 1m and a length scale ranging from 100 km to 10000 km. The sharpest gradients occur at the strong western boundary currents such as the Gulf Stream or the Kurshio. At a western boundary current a one meter head rises in roughly 100km. The return flow is distributed across the remaining ocean basin, i.e., the return flow represents a 1 meter drop over 10000 km. Therefore the mean circulation is only a factor near the strong western boundary currents. Approaches to simultaneously determine the geoid and the ocean circulation using altimeter, gravity, and hydrographic data have been discussed (Wunsch, 1978; Wunsch & Gaposchkin, 1980). At present the very long wavelength features of the circulation are being investigated with Seasat-1 altimeter data using a satellite derived geoid as a reference (Tai & Wunsch, 1983). However, this remains probably the most challenging and complex interdisciplinary problem in Altimetric Oceanography.

VIII.2 The Eddy Field

Superimposed on the mean circulation is a variability with one component labeled the Mesoscale Eddy Field. Many discussions make a distinction between cold cyclones (rings) and eddies. The former are analagous to

weather cyclones and are believed to originate from similar dynamical phenomena. There is not yet any understanding of the generation of eddies. They may be rings that have traveled great distances, or be generated by unstable interactions of the flow and bottom topography. The flow field associated with surface eddies can extend below 3km. Rings are thought to have a lifetime of two to three years. It is thought that about five rings are formed each year from the Gulf Stream. Therefore we expect to find about 15 rings in the Western North Atlantic at any time. As emphasized by Koshlyakov & Monin (1978), the North Pacific is even more complex.

Rings and eddy fields are broadly characterized with a 1 to 2m amplitude, a 10 to 30cm variance, a 150km to 250km horizontal wavelength, and a time constant of 2 to 5 months (Fu, 1982; Koshlyakov & Monin, 1978; Douglas & Cheney, 1981). By this time constant we mean that the variability will move by one wavelength in one time constant. Put another way, one can hope to average the mesoscale eddy field over one time constant. Unfortunately, the ocean variability is thought to have components with decade time constants, and possibly longer. The oceanographic data are not yet sufficient to constrain the period of oceanographic variability (Wunsch, 1983). Therefore the analysis of altimetric data must be hardened against this possible low frequency oceanographic variability.

To quantify eddy field averaging, we can use the description of the eddy field in terms of Rossby Waves resulting from Baroclinic Instability. The theory predicts the phase velocity of propagation c as:

$$c = \beta \lambda^2 / 2$$

where:

$$\beta = 2 \Omega \cos \phi / a_e$$

and

λ is the wavelength (peak to trough)

Ω is the rotation rate of the earth ($0.727 \times 10^{-4} \text{ sec}^{-1}$)

ϕ is the latitude

a_e is the earth radius

The baroclinic Rossby Radius of deformation:

$$\lambda_R = \sqrt{gh} / f$$

where

$$f = 2 \Omega \sin \phi$$

and g is the acceleration of gravity, h is the height (head) of the rotating system free surface. The Rossby Radius is the shortest distance over which geostrophic flows of any significance can occur. At mid latitude for a height of 1m, $\lambda_R = 31\text{km}$. Of course, for a given height, longer wavelengths exist.

We can calculate the time for a Rossby Wave (eddy) to travel one wavelength as:

$$P = \frac{\lambda}{c} = \frac{2}{\beta \lambda} = \frac{a_e}{\Omega \cos \phi \lambda}$$

and for the shortest wavelength of a Rossby Radius:

$$P_R = \frac{2 a_e}{\sqrt{gh}} \tan \phi$$

Now, for a mission duration, T , and with uniform sampling, each eddy will move $n=T/P$ wavelengths. Therefore the error, after averaging, will be h/\sqrt{n} , i.e.

$$E = \sqrt{\frac{a_e}{T \Omega \cos \phi}} \frac{h}{\sqrt{\lambda}}$$

and for a Rossby Radius Wave:

$$E_R = \sqrt{\frac{2 a_e}{T} \tan \phi} \frac{h^{3/4}}{g^{1/4}}$$

We give in Table 6 some sample values, for a mission of $T=2$ years, and $\sin \phi = \cos \phi = 1/\sqrt{2}$.

TABLE 6
 AVERAGING OF EDDY FIELD
 TWO YEAR MISSION
 LATITUDE = 45 DEG.

<u>h</u> (cm)	<u>λ</u> (km)	<u>error</u> (cm)
100	31.3*	25
50	22.0*	15
100	100	12
100	200	8

*Rossby Radius corresponding to h.

If we average all the altimetric data, over as long a time base as possible, we define a mean surface in this way. The availability of a 10 year time base using the, admittedly less accurate, Geos-3 data is an advantage. This average surface would contain a mean circulation which could be removed with any number of models, e.g., Tai & Wunsch (1983), the Steric Anomaly field of Wyrтки (1974, 1975), or Levitus & Oort (1977). For the moment any such model must be viewed with caution as it will inevitably be built on some assumptions. One such assumption is the level of no motion which is certainly not correct; see e.g., Wunsch (1978). From the geodetic viewpoint, this oceanographic signal will be considered as part of the error budget for some time to come. Only continued fundamental oceanographic research, an oceanographic research satellite such as TOPEX (Wunsch, 1981), or a dedicated Gravity Satellite such as GRM (Kaula, 1983) will significantly change this situation.

IX.

ENVIRONMENTAL CORRECTIONS, A SURVEY

The environmental contributions to the observations include:

- hw, the wet tropospheric correction
- hd, the dry tropospheric correction
- hb, the inverse barometer correction
- hi, the ionosphere correction
- he, the solid earth tide correction
- ho, the ocean tide correction
- hs, the significant wave height correction

There is general agreement that tide models for h_e have an error less than 2 cm. Ocean tide models (h_o), (e.g., Schwiderski, 1982a, b, c; Parke & Henderschott, 1980; Parke, 1980) are generally better than 10 cm, where applicable. Parke & Henderschott (1980) is primarily a deep sea model, whereas Schwiderski (1982a,b,c) would be more appropriate near coasts where tide gauges exist. The model accuracy in regions without tide gage measurements is unknown. There is therefore a possible true variable error source with a wavelength between 500km and 1000km (Tapley, et al 1983).

With suitable care, the ionosphere correction can be modeled with an accuracy better than 2 cm, as described by Lorell et al (1983). Of course a dual frequency altimeter would have measured this correction directly.

The inverse barometer correction (h_b) corresponds to the depression (approximately 1cm/mbar) of the sea surface with change in atmospheric pressure. This is the order of 25 cm with a time constant of approximately two days, i.e., the time constant of oceanospheric response is about 48 hours. Except near storms or other transient phenomena, the

FNOC averaged global pressure field will provide the necessary correction.

The dry troposphere correction (h_d) has an amplitude of approximately 2.1 m. The surface pressure available from the FNOC is adequate to compute this correction with 1 or 2 cm accuracy. In fact a comparison of FNOC data with radiosonde data show an agreement of 0.59 cm rms for this dry troposphere correction (Tapley et al 1983).

The wet troposphere correction (h_w) can exceed 40 cm, with a length scale of 150 to 500 km. On Seasat-1, the Scanning Multichannel Microwave Radiometer (SMMR) provided data to compute this correction with an RMS of 2.7 cm rms. The use of FNOC data for computing this correction is the subject of the remainder of this report. The accuracy that can be obtained using FNOC, averaged over several months, can be approximately 2 cm, and will not preclude obtaining a mean ocean surface with an accuracy better than 5 cm.

The accuracy of the SMMR wet troposphere correction (h_w) is 2.79 cm rms, as obtained in comparison with radiosonde data (Tapley et al 1982b). The FNOC derived data was also discussed and shown to have an accuracy of 5.73 cm rms. The SMMR had a horizontal resolution of about 40 km. The FNOC information is based on hindcast models with a grid spacing of several hundred kilometers. Furthermore data on which the for FNOC models are based is less complete in the southern hemisphere. One would expect the FNOC derived correction to be less accurate. The remainder of this report is concerned with quantifying the wet troposphere correction further, and examining how well one can expect to make this correction in the absence of SMMR, or equivalent data.

X.

TROPOSPHERIC REFRACTION

X.1 Basic Principles

The increase in time delay of electromagnetic waves depends on the index of refraction n . The velocity (v) of propagation, $v=c/n$, where c is the speed of light. In the case of the troposphere the index of refraction is nondispersive for frequencies below the 22.5 GHz water vapor absorption line. The Seasat altimeter operates at a single frequency of 13.5 GHz. Therefore the group, phase, and signal velocities are all the same and are less than c .

The index of refraction can be written (Bean & Dutton, 1966);

$$n = 1 + N$$

where

$$N = (n-1) = \left[77.6 \frac{P(z)}{T(z)} + 3.73 \times 10^{-5} \frac{e(z)}{T^2(z)} \right] \times 10^{-6}$$

where; z is the height in question, $P(z)$ is the atmospheric pressure in millibars, $T(z)$ is the temperature in degrees Kelvin, $e(z)$ is the partial pressure of water vapor in millibars, and the constants 77.6 and 3.73×10^{-5} depend on the average global atmospheric composition near the earth's surface. The total time delay of a radar pulse, assuming vertical propagation, is:

$$\Delta T = \int_{z=0}^{z_{\text{sat}}} \frac{dz}{v} = \frac{1}{c} \int_{z=0}^{z_{\text{sat}}} n \, dz = \frac{1}{c} \int_{z=0}^{z_{\text{sat}}} (1 + N) \, dz$$

Since the troposphere extends to altitude Z_t , the measured time delay converted to distance $h=c \, (dt)$

$$h = \int_0^{z_{\text{sat}}} dz + \int_0^{z_t} N \, dz$$

where the first term is the geometric distance, i.e., based on the vacuum delay (h_v) and the second term (h_t) is the additional delay due to the troposphere. Now:

$$10^6 h_t = 77.6 \int_0^{z_t} \frac{P(z)}{T(z)} \, dz + 3.73 \times 10^5 \int_0^{z_t} \frac{e(z)}{T^2(z)} \, dz$$

and $h_t = h_d + h_w$. The first term is known as the dry term, and is evaluated assuming the atmosphere obeys the perfect gas law and is in hydrostatic equilibrium, as:

$$h_d = 2.277 \times 10^{-3} \left[1 + 0.0026 \cos(2\varphi) \right] P_0$$

where P_0 is the atmospheric pressure at the surface and φ is the latitude (geodetic). The second term accounts for the variation of surface gravity. Using the same assumptions, that the temperature decreases linearly above the ocean, and that;

$$e(z) = \left[\frac{T(z)}{T_0} \right]^\alpha$$

The second term can be integrated to:

$$h_w = 2.277 \times 10^{-3} \left[\frac{1255}{T_0} + 0.05 \right] e_0$$

where e_0 and T_0 are respectively, the partial pressure water vapor in millibars and temperature of the atmosphere in degrees Kelvin at the surface.

The SMMR on Seasat recorded antenna temperatures at 18, 21, and 37 GHz with both horizontal and vertical polarization. Based on the development of Wisler & Hollinger (1977) the wet troposphere range correction can be expressed as:

$$R = R_0 + \gamma \sum_{i=1}^6 \alpha_i (B_i - B_i^0)$$

where R is the range correction, are constants, B_i are the brightness temperatures, B_i^0 are the reference brightness temperatures, R_0 is the reference range correction, and γ is an adjustable scale parameter.

In the Seasat-1 case α_i and B_i^0 were adopted from Hollinger & Wisler and the (2) parameters R_0 and γ were determined using radiosonde data obtained at times coincident with Seasat-1 overflights (Tapley et al 1982). Sixteen (16) values from four geographical locations (Kwajalin, Bermuda, and Ships Endurer and Hecla) were used giving $R_0=11.73 (\pm 0.12)$ cm and $\gamma=1.29 (\pm 0.0008)$ with a residual standard deviation of 2.79 cm. It should be emphasized that the data are small in number (16 points) and

that the observations had either small or large for atmospheric water vapour: there is a lack of values in the mid moisture range. Finally, the data from a fifth site (Majuro) were deleted because they gave inconsistent results. Since more radiosonde data corresponding to Seasat-1 tracks is now available, the SMMR calibration of water vapor could be discussed more fully. If the Seasat-1 data have anomalies, apparently connected with wet troposphere corrections, this would be a fruitful avenue of investigation. In any event we proceed assuming that, where SMMR data is available, the water vapor correction (hw) is known with an accuracy of 2.79 cm rms. In the same report (Tapley et al 1982), a comparison of 13 FNOC derived hw corrections indicate they have an accuracy of 5.72 cm rms.

In what follows we compare all SMMR, $h(SMMR)$, and FNOC, $h(FNOC)$, corrections assuming the SMMR values are correct. There are three questions in mind:

- 1) On average how good is the FNOC correction?
- 2) Are there regional variations?
- 3) How good is the average variation when used for the correction?

X.2 The Seasat SMMR Data Analyzed

All available Seasat data in the western North Atlantic (20N - 60N, 270W - 330W) was requested from the NOAA/EDIS. This data was provided on one 1600 BPI magnetic tape as described in Lorell et al (1980). All the $h(SMMR)$ and $h(FNOC)$ data with the latitude and longitude were culled from the data. Only observations where both values were provided were used. The resulting 132298 observations were used for comparison. The $h(SMMR)$

ard $h(\text{FNOC})$ agreed to 4.097 cm rms with a mean difference of 0.040 cm. Thus to first order one can conclude that the $h(\text{SMMR})$ correction and average meteorological data are in excellent agreement. Further, the use of $h(\text{FNOC})$ in the Western North Atlantic is quite acceptable. If we adopt 2.79 cm rms (Tapley et al, 1982) as the accuracy of $h(\text{SMMR})$ and assume errors in the two data sets are uncorrelated, then the $h(\text{FNOC})$ would have an accuracy of 2.94 cm rms.

X.3 The Regional Variation of Wet Troposphere Correction

For the use of satellite to sea surface altimetry for determination of the mean sea surface will use all available data. Therefore, one is interested in the geographical variation of this correction, its error, and the autocorrelation function of the error. In other words, we ask what the error in the average sea surface height would be using $h(\text{FNOC})$, assuming the $h(\text{SMMR})$ to be correct, as a function of position and what is its autocorrelation function. To address this question, a data base was formed taking the average SMMR correction and the average FNOC correction for a grid. A 15' x 15' (27km x 27km) grid was selected. This grid is more coarse than the altimeter data spacing (7 to 15 km), finer than the SMMR resolution (40 km) or the FNOC resolution (250 km), and approximately the desired resolution of the final geodetic product. This data base was used for the remainder of this analysis.

To discover any regional variation in hw , the mean SMMR data was again averaged in 2deg x 2deg squares. This was a weighted average based on all observations in the 2deg x 2deg region rather than a simple mean of the 15' x 15' values. Figure 1 is a number map of these values. Also on the

number map is a rough outline of the North American Continent. There are altimeter measurements from The Great Lakes, St. Lawrence River, Hudson's Bay and other water surfaces. These observations are small in number and do not affect the overall statistics. The agreement of the FNOC and SMMR data for these overland regions is good. Of course, these values will not contribute to determination of the marine geoid because these bodies of water are not at the same potential as mean sea level. Evidently there is a broad latitude dependence in the wet troposphere correction, with a less pronounced longitude dependence. The latitude dependence accounts for 94% of the variance in the $h(\text{SMMR})$. For each 15' band of latitude, the mean was taken. Figure 2 is a plot of the latitude dependence. The latitude dependence of the $h(\text{FNOC})$ is virtually identical. Furthermore, for each latitude the variance of the difference between the signal and the mean was calculated and is plotted in Figure 3. This variance represents the wet troposphere information not included in the mean given in Figure 2. The agreement is between 3 and 6 cm rms, indicating that using a latitude dependent mean h_w would give troposphere corrections with an accuracy of 5 cm rms. Figure 3 is plotted on the same scale as Figure 2 to demonstrate the remarkable fit of the mean troposphere correction. Also, we see that the FNOC data is sufficiently good to determine this latitude dependent function, at least in the Western North Atlantic.

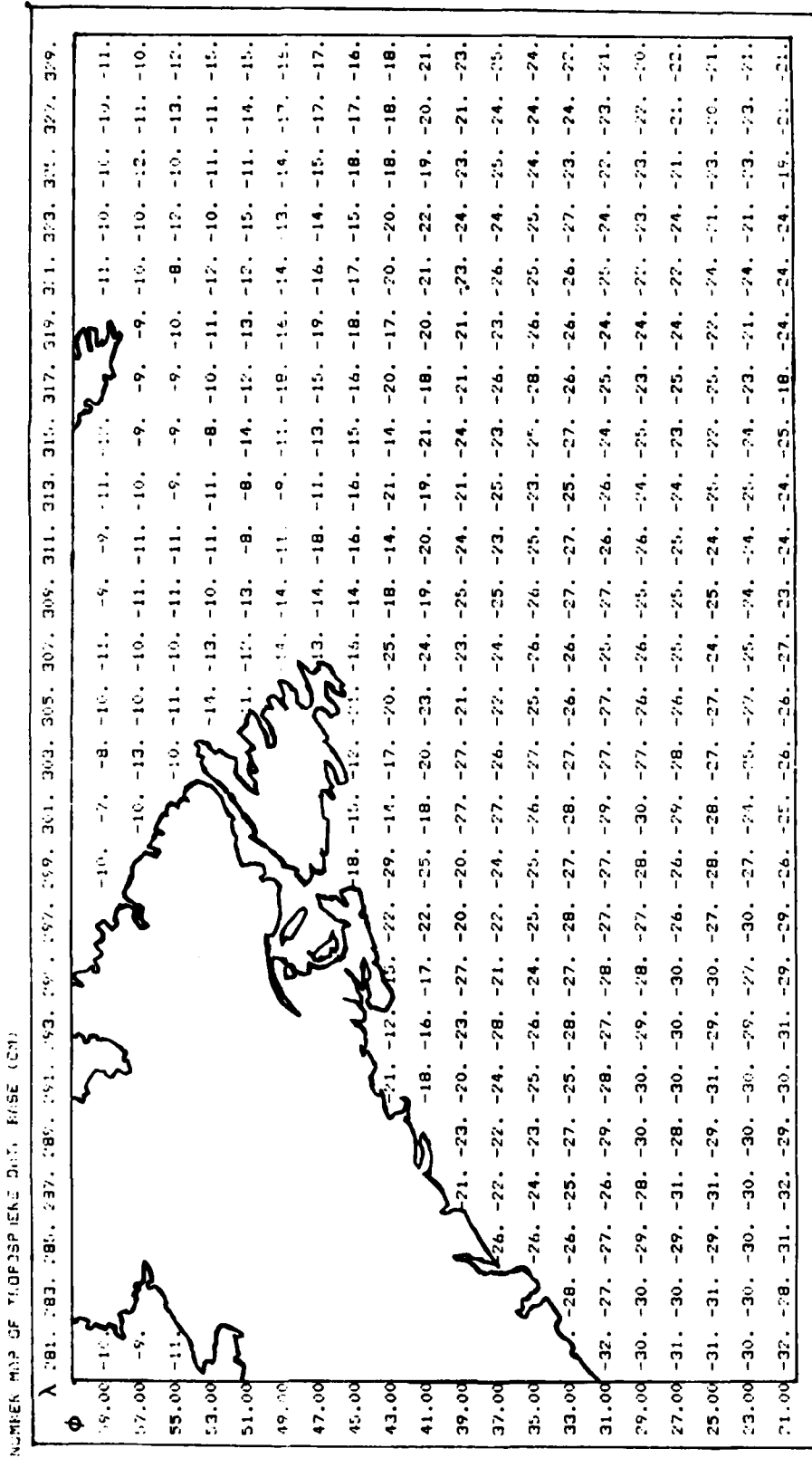


Figure 1. Number Map of Wet Troposphere Correction, Western North Atlantic -- 2 deg x 2 deg means (cm)

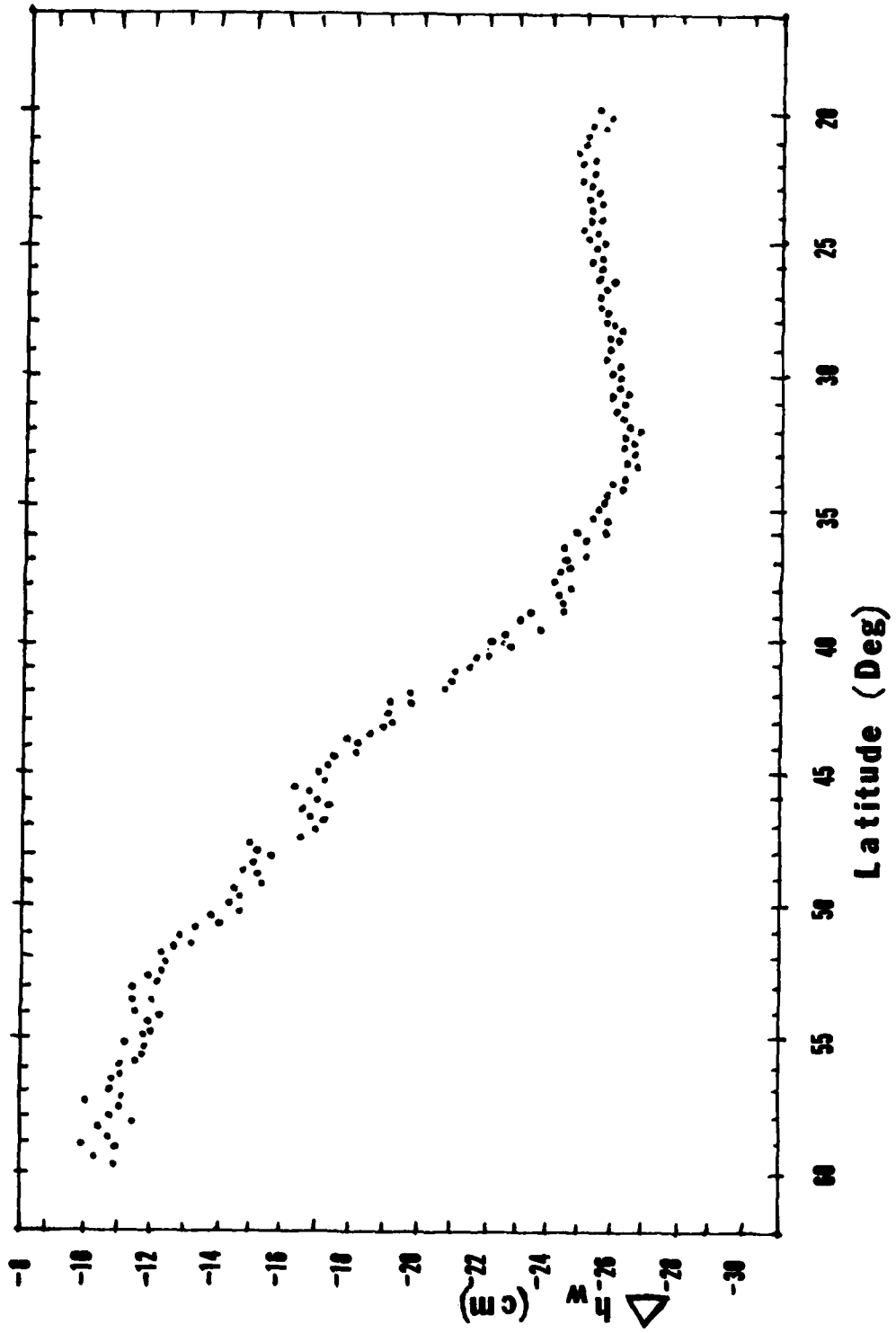


Figure 2. Mean Wet Troposphere Correction, 15' Latitude Bands, Western North Atlantic

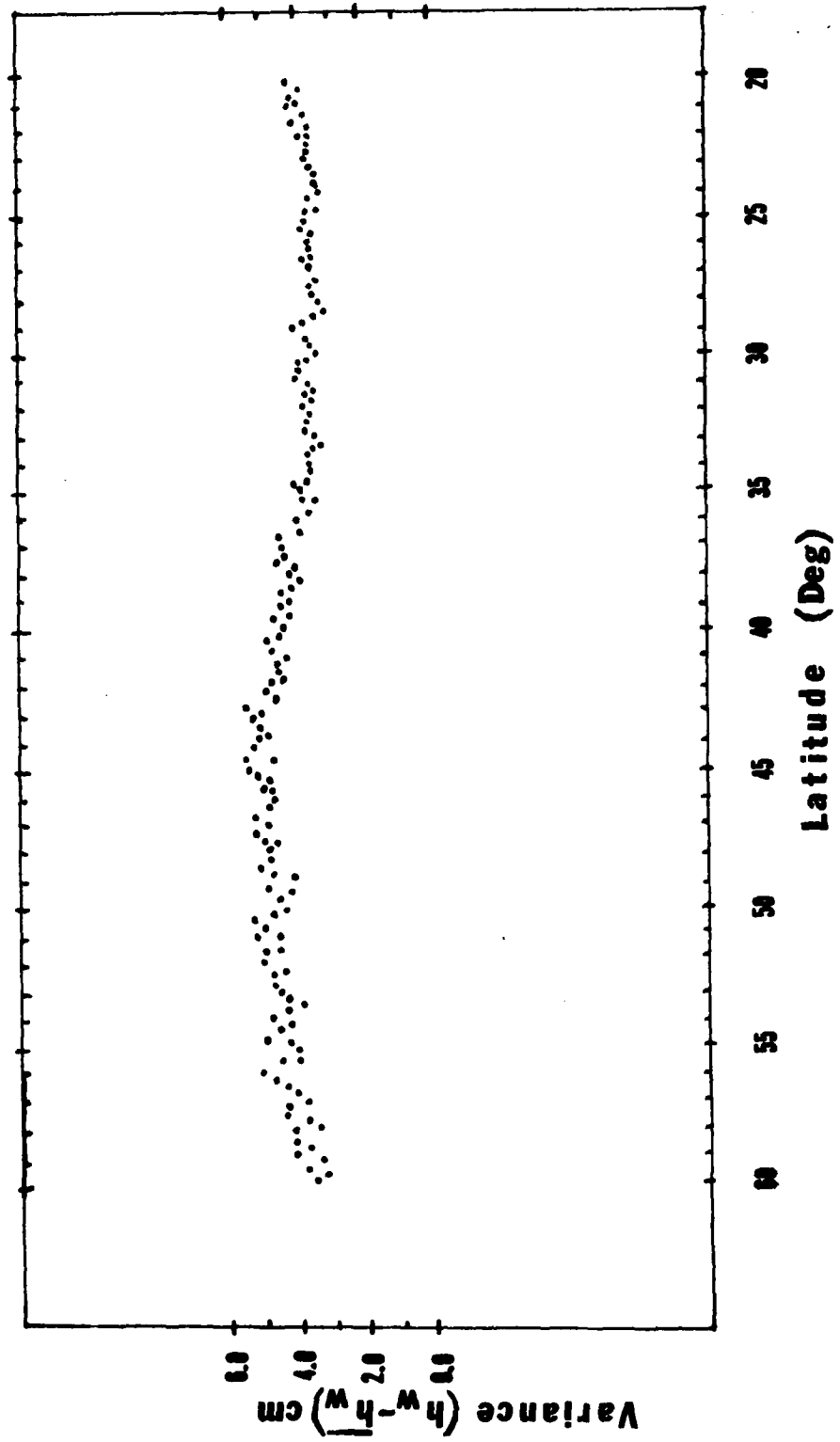


Figure 3. Variance of Wet Troposphere Correction with Respect to Mean Latitude Variation, Western North Atlantic

X.4 Spectra of Wet Troposphere Correction

Finally, we consider the variance and autocovariance of the SMMR and FNOC derived tropospheric corrections and their difference with respect to the mean latitude dependent h_w correction ($H=H(\phi)$). The $h(\text{SMMR})$ variance represents the true information h_w and would be an estimate of the error committed ignoring the h_w correction. The $h(\text{SMMR})-H$ variance represents the error in H . The $h(\text{FNOC})-H$ represents the amount of short wavelength information actually present in the FNOC data. Finally, the variance of the difference, $h(\text{FNOC})-h(\text{SMMR})$, would represent the error in mean sea surface if the FNOC correction were to be used. The basic results are summarized in Table 7.

TABLE 7
STATISTICS OF SMMR AND FNOC DATA

$\langle h(\text{SMMR})^{**2} \rangle$	= 506.	cm**2	= (22.5cm)**2
$\langle h(\text{FNOC})^{**2} \rangle$	= 491.	cm**2	= (22.2cm)**2
$\langle (h(\text{SMMR})-H)^{**2} \rangle$	= 20.03	cm**2	= (4.48cm)**2
$\langle (h(\text{FNOC})-H)^{**2} \rangle$	= 5.29	cm**2	= (2.3 cm)**2
$\langle (h(\text{FNOC})-h(\text{SMMR}))^{**2} \rangle$	= 15.53	cm**2	= (3.94cm)**2

The autocovariance functions are presented in Figures 4, 5, and 6. The tabular data are given in Table 8. The small value of $\langle (h(\text{SMMR})-h(\text{FNOC}))^{**2} \rangle$ is consistent with a meteorological hindcast with coarse grid spacing. It also reemphasizes the notion that mean regional values are almost as good as the detailed FNOC or SMMR values in a statistical sense. The very rapid decrease in the $h(\text{SMMR})$ autocorrelation function indicates that when spatially averaged, the departure from the mean (H) is very close to a random, uncorrelated signal. The error in the FNOC is only slightly less than this ignored signal.

TABLE 8
 AUTOCOVARIANCE FUNCTIONS

h(SMMR)		h(FNOC)		h(SMMR)-h(FNOC)	
<u>C(TAU)</u>	<u>TAU(deg)</u>	<u>C(TAU)</u>	<u>TAU(deg)</u>	<u>C(TAU)</u>	<u>TAU(deg)</u>
1.000	0.000	1.000	0.000	1.000	0.000
0.480	0.034	0.538	0.034	0.316	0.034
0.286	0.393	0.449	0.393	0.280	0.393
0.275	0.618	0.449	0.618	0.266	0.618
0.125	0.872	0.302	0.872	0.153	0.872
0.090	1.124	0.300	1.124	0.109	1.124
0.080	1.374	0.282	1.374	0.099	1.374
0.061	1.624	0.258	1.624	0.079	1.624
0.070	1.873	0.261	1.873	0.078	1.873
0.086	2.125	0.283	2.125	0.085	2.125
0.095	2.373	0.298	2.373	0.072	2.373
0.085	2.622	0.316	2.622	0.063	2.622
0.071	2.874	0.302	2.874	0.069	2.874
0.070	3.124	0.277	3.124	0.077	3.124
0.067	3.375	0.268	3.375	0.072	3.375
0.074	3.627	0.252	3.627	0.082	3.627
0.093	3.878	0.261	3.878	0.098	3.878
0.094	4.127	0.264	4.127	0.096	4.127
0.098	4.376	0.258	4.376	0.101	4.376
0.093	4.624	0.237	4.624	0.109	4.624
0.097	4.874	0.222	4.874	0.122	4.874

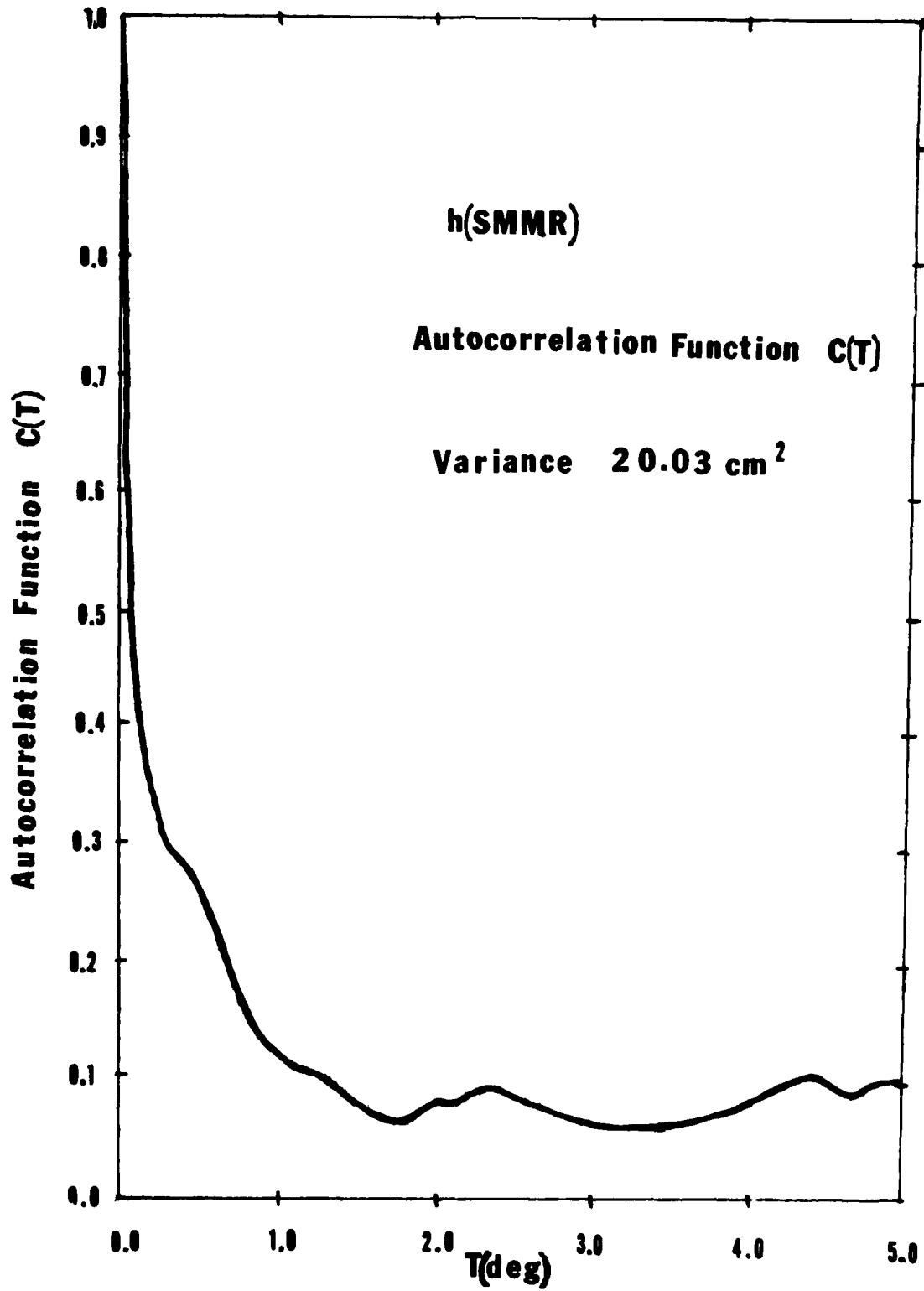


Figure 4. Autocorrelation Function for h(SMMR).

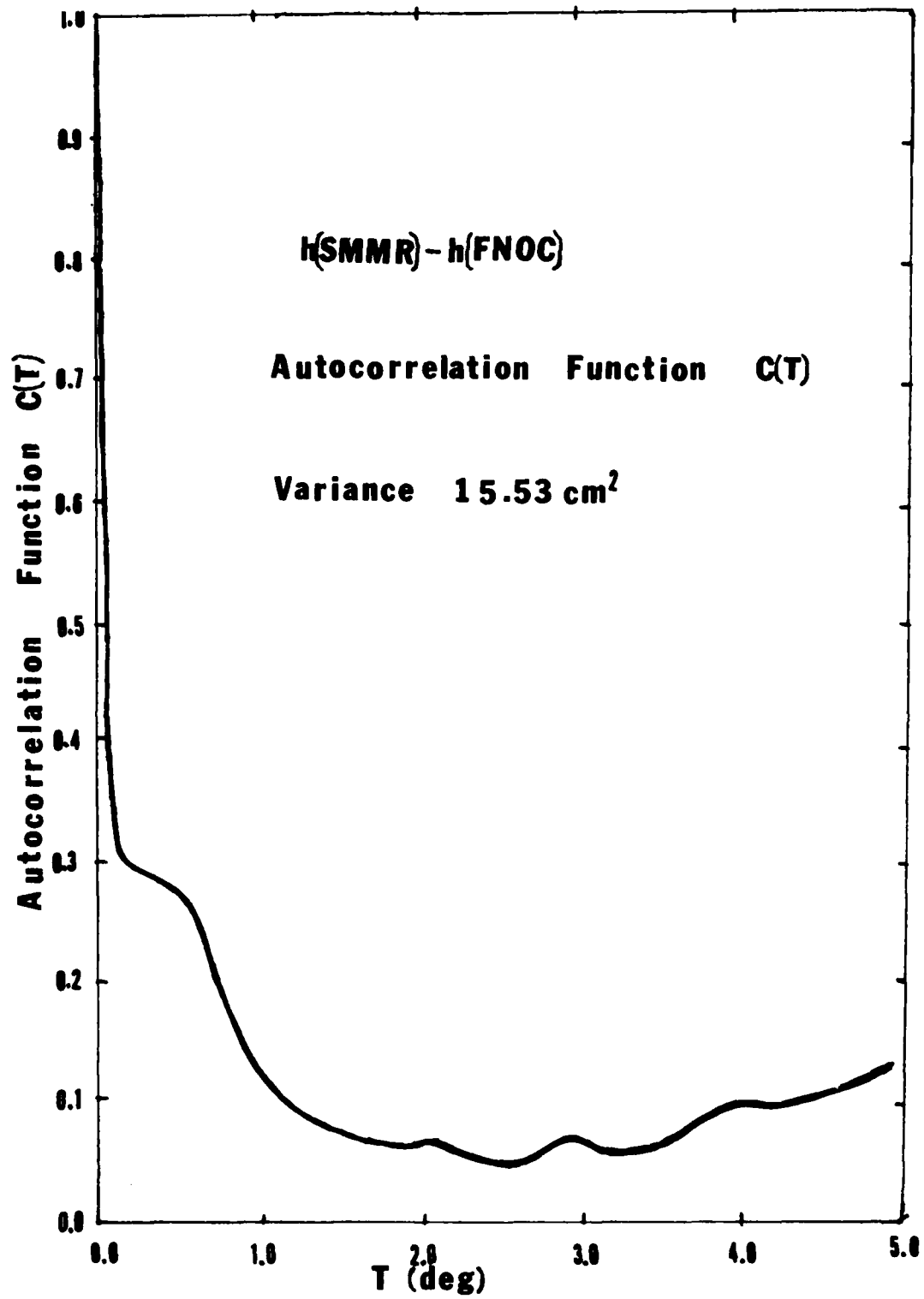


Figure 5. Autocorrelation Function for h(FNOC).

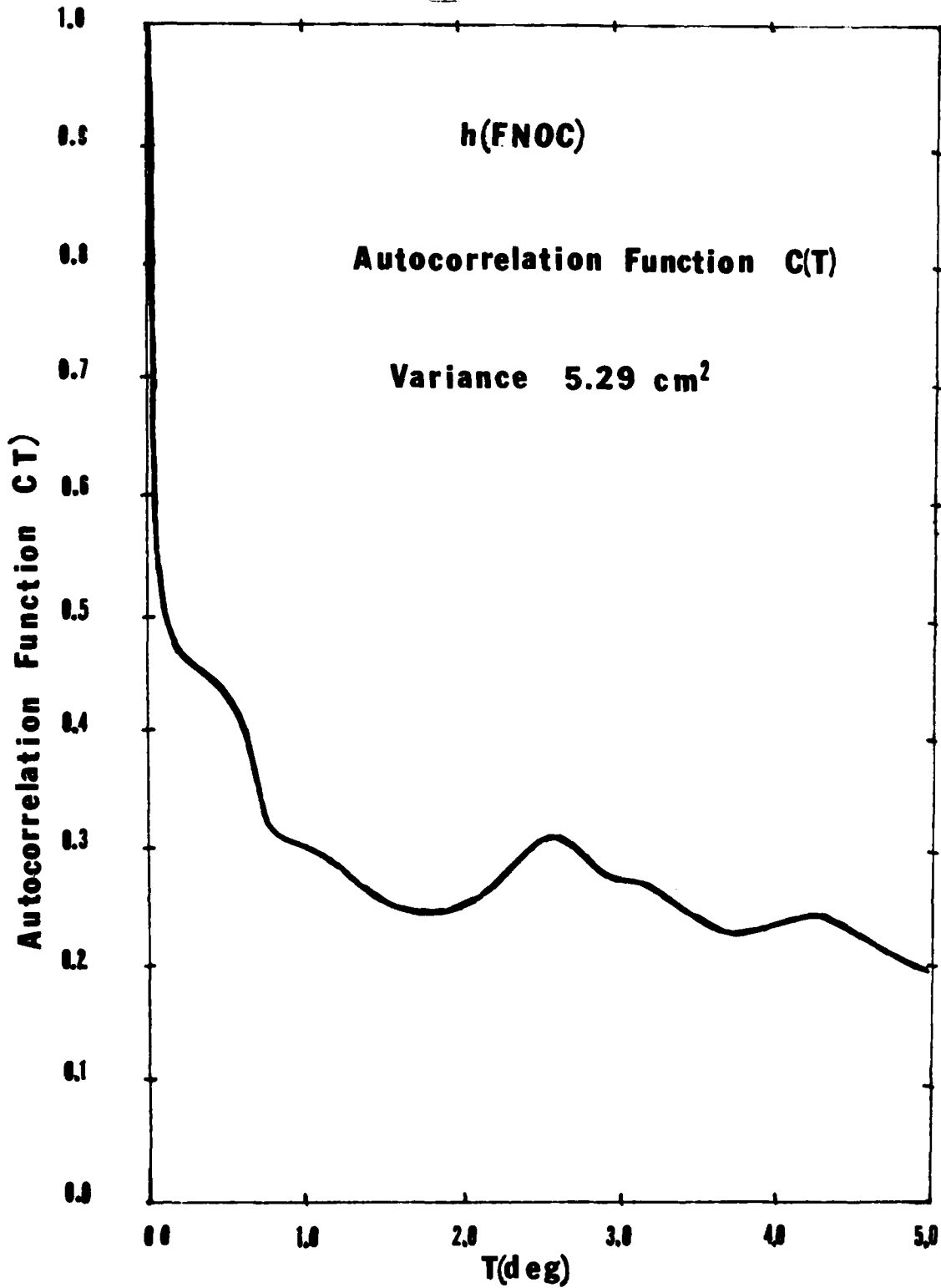


Figure 6. Autocorrelation Function for h(FNOC)-h(SMMR).

These results are an average for all 15' x 15' squares containing one or more data points. This data set was obtained in approximately 90 days. Some squares have many more observations than others, and we can inquire if the uncertainty improves as the number of data points increases. Figure 7 plots the rms error as a function of the number of data points in the mean. By far the largest number of squares had 1, 2 or 3 data points, and these dominate the overall sigma. However, for squares with 15 or more data points, the sigma is approximately $(2.25 \text{ cm})^{**2}$. There does not seem to be much further improvement as the number of data points increases. It is unclear why. However, with the two year lifetime of Geosat-A one can reasonably expect to have all squares observed more than 15 times. Of course, the actual distribution of ground tracks depends on the details of the satellite manoeuvres and on other programmatic considerations. From the point of view of averaging the wet troposphere error one should obtain as uniform a geographical distribution as possible.

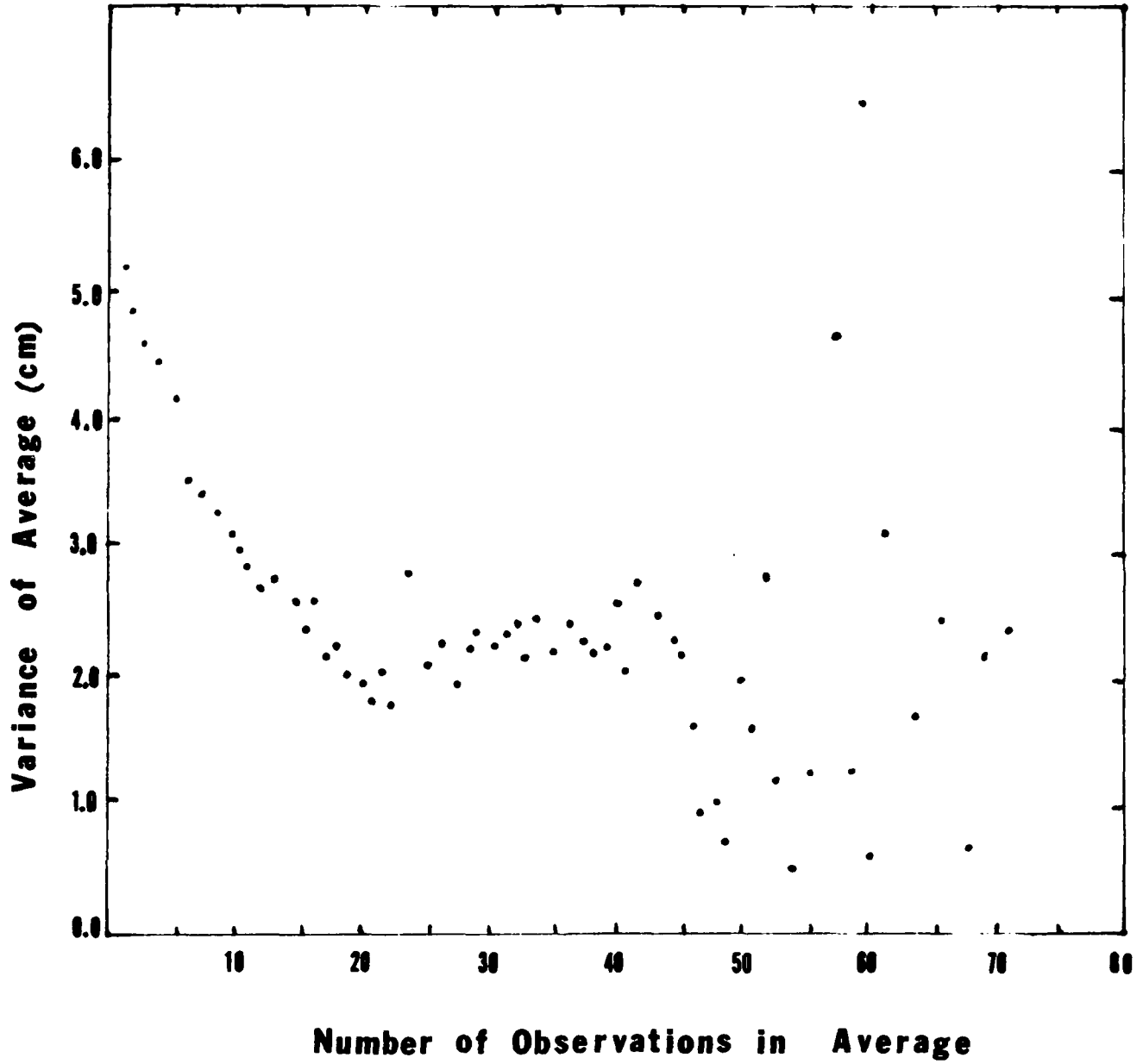


Figure 7. Error of 15' x 15' Square as Function of Number of Observations in Average.

X.5 Discussion of Wet Troposphere Error

We have taken the Seasat-1 data set in the Western North Atlantic to compare the wet troposphere correction derived from the SMMR and that derived from the FNOG data. The SMMR data is believed to have an accuracy of 2.67 cm rms and is used as the standard of comparison. The objective here is to project the situation for Geosat-A which will not be equipped with a SMMR, and will therefore depend on FNOG for this data.

This study is limited in three ways. First, it assumes the Seasat-1 SMMR is a suitable standard of comparison. Recall that the SMMR calibration was made with only 16 radiosonde data sets, 16% of the data was rejected, and even so had a rms of 2.67 cm. However, the agreement in the analysis reported here, of the mean, the variance, and the geographical dependence of the SMMR and FNOG data would support confidence in the SMMR. This issue can be resolved by investigation of additional available radiosonde data.

Second, the analysis is limited to the Western North Atlantic where the FNOG data would be the best available. In most other oceanic regions one would expect poorer quality of the FNOG hindcasts. However, since the flight of Seasat-1 in 1978 the general quality of the FNOG hindcast can be expected to improve. This can be discussed further by analyzing the remaining Seasat-1 data and a general examination of the FNOG data products. In particular the geographical mean wet troposphere correction should be obtained for each of the world's oceans.

Third, and finally, the data was taken in the three month period (July - October 1978). During this summer time interval (the dog days or summer doldrums), one would expect smoother changes than one would during the winter. Therefore the variability present in this data might be more

benign than usual. Furthermore, the short time interval precludes investigation of seasonal variations in the mean tropospheric correction and its variance. This seasonal variation must exist and be important. Seasonal variation of the mean geographical variation can be investigated using FNOG data.

Within these caveats, one can conclude that using the FNOG derived wet troposphere correction will, in a statistical sense, contribute an error of $(3.94 \text{ cm})^2$ for a Seasat-1 type of data span. With a full two years, which could provide 14 points in each $15' \times 15'$ equatorial square after two years, one can anticipate a troposphere error of $(2.25 \text{ cm})^2$.

To verify and insure this encouraging result, a number of steps should be taken:

- 1) The full set of Seasat SMMR and FNOG data should be analyzed to obtain an initial estimate of the regional distribution of the mean wet troposphere correction.

- 2) The accuracy of the FNOG data in other oceans should be examined and regions of deficient coverage studied.

- 3) Regional and seasonal models of the wet tropospheric correction should be developed for parts of the ocean where the FNOG data does not give satisfactory agreement.

- 4) The Seasat SMMR calibration can be redetermined following the procedure of Tapley et al (1982). However, it is not anticipated that significant changes in the calibration will occur, though a more reliable (in the sense of more samples) estimate of the accuracy of the SMMR calibration will be achieved.

XI.

SUMMARY

We have investigated the accuracy which can be expected using Geosat-A satellite to sea surface radar altimeter data for determination of the mean sea surface in terms of the ultimate objective: viz, determining the marine geoid and gravity at sea. This view allows one to concentrate on regional, intermediate wavelength, time invariant error sources. This is important because some error sources that have long wavelength errors along a track (e.g., Orbit errors) have random (white) spectra when averaged over space, i.e., when viewed across track-to-track. Other error sources have long wavelength but move geographically, and have a similar random contribution when averaged over time, i.e., when viewed along colinear tracks. The benefits of averaging do not eliminate the desirability of modeling all effects with utmost care. Clearly one would not want to rely on a statistical improvement if not necessary. Listed in Table 9 are the Altimeter Data error sources discussed. We have already discussed the errors in computing gravity anomalies as a function of geoid height (Sections II, IV, V, VI; and Gaposchkin, 1983).

We assume that clean data is available, i.e., that instrument glitches, saturation, specular returns, etc., are already removed. Furthermore, we assume that sensor bias depending on significant wave height, and attitude are properly calibrated. In this case, the two large error sources in Table 6 are the orbit error, and the mesoscale eddy field. Note that we believe that a third error source of concern, that due to the wet troposphere correction, does not seem to be a problem.

The orbit error has been discussed above. This presents a major challenge. No doubt by application of methods described above, significant progress can be expected. Nevertheless, it would seem unwise to assume an orbit error much better than 10cm along any given track. If this is achieved, then the track-to-track averaging could improve this by about a factor of two to three. Therefore we can hope for a random component to the orbit error of 3 to 5 cm.

The ocean tide models are quite good in regions where tide gauge data is available. The 10 cm uncertainty is really conservative. This is all one can say in the absence of additional information. However, the tidal signal is time variable at a given location. Therefore, even if there was no progress in tide modeling, which is unlikely, the natural time averaging for an individual region over the lifetime of Geosat-A would reduce this error source to less than 2cm. Of course there will certainly be local regions with large tidal signals that will not be modeled this well.

The main obstacle to complete use of satellite altimeter data to determination of the marine geoid is oceanographic phenomena that cause the sea surface to differ from the geoid. Such phenomena have amplitudes of a meter, temporal frequencies of days to decades, and spatial frequencies of 50km to ocean basin scale, 10000km. The mean circulation can be eliminated by avoiding the geographical regions of the strong Western Boundary Currents such as the Gulf Stream or Kurshio. The ubiquitous Mesoscale Eddy field can be approached in two ways. First, by using the natural 2 to 5 month time constant, averaging over the full two year Geosat-A lifetime, one can reduce this 100 cm time variable signal to between 8 and 25 cm rms. Second, by using colinear tracks and simple models of an eddy one can map the pro-

gress of the eddy field. With an eddy model, matched filters could be successful in a way similar to the study of seamounts with Seasat-1 data. If successful, this model can be subtracted from the altimeter data before it is averaged for a mean sea surface.

Principal Recommendations

1. Establish the global geographical and seasonal variation of the wet troposphere water vapor correction using the Seasat-1 data and a longer time base of data from FNOC.
2. Develop models for Mesoscale Eddies and use Seasat-1 as a test for technique development to map the evolution of the eddy field.

TABLE 9
ERROR BUDGET FOR GEOSAT-A

<u>Phenomena</u>	<u>Error of Single Measurement (cm)</u>	<u>Error Averaged Over Mission (cm)</u>
Altimeter Noise	2.5	-
Sea State Bias (2% h1/3)	2. - 5.	-
Troposphere dry	0.7	-
Troposphere wet*	5.0	2.2
Ionosphere	3.0	-
Orbit error**	10.0	3. - 5.
Inverted Barometer	3.0	-
Solid Body Tide	2.0	-
Ocean Tide	2. - 10.	2.0
Mean Ocean Circulation***	100.	100.
Eddy Field	100.	8. - 25.

*Assumes FNOC derived correction.

**Assumes Crossing Arc Orbit Rectification.

***Only Near Western Boundary Currents.

XII.

ACKNOWLEDGEMENTS

This analysis was supported by Air Force Geophysics Laboratory Contract F19628-82-C-0144. We also thank Mr. Lew Decker, DMAAC, for providing a computer implementation of the Molodensky Integral used for part of the analysis, and for his encouragement in pursuing these investigations.

XIII.

REFERENCES

- Anderle, R. J., & Hoskin, R. L.; 1977 Correlated Errors in Satellite Altimetry Geoids, *Geophys. Res. Lett.*, Vol. 4, pp. 421-423.
- Bean, B. R., & Dutton, E. J.; 1966, *Radio Meteorology*, NBS Monogr. 92, 465 pp., March 1966.
- Born, G. H., Richards, M. A., & Rosborough, G. W.; 1982, An Empirical Determination of the Effects of Sea State Bias on SEASAT Altimetry, *Journ. Geophys. Res.*, Vol. 87, No. C5, pp. 3221-3226, April 1982.
- Buglia, J. J., 1976, The Effect of Remote Zones of the Accuracy of Evaluating the Molodensky Integral, NASA TM X-72798, Langley Research Center, Hampton, Virginia 23665, 21 pp.
- Cheney, R. E., & Marsh, J. G.; 1981, Oceanic Eddy Variability Measured by Geos-3 Altimeter Crossover Differences, *EOS*, Vol. 62, No. 45, pp. 743-752, November 10, 1981.
- Cloutier, J. R.; 1981, A New Technique for Correcting Satellite Ephemeris Errors Indirectly Observed From Radar Altimetry, TR-246, Naval Oceanographic Office, NSTL Station, Bay St. Louis, MS 39522, pp. 64, April 1981.
- Douglas, B. C., & Cheney, R. E.; 1981, Ocean Mesoscale Variability From Repeat Tracks of Geos-3 Altimeter Data, *Journ. Geophys. Res.*, Vol. 86, No. C11, pp. 10931-10937.
- Fu, L.; 1982, On the Wavenumber Spectrum of Oceanic Mesoscale Variability Observed by the Seasat Altimeter, Preprint, Jet Propulsion Laboratory, Pasadena, CA 91109, 40 pp., October 1982.
- Gaposchkin, E. M.; 1983, Accuracy of the Molodensky Integral, TMO01, MATHEMATICAL GEOSCIENCES INC., Lexington, Mass. 02173, 23 pp.
- Hayne, G. S., & Hancock, D. W.; 1982, Sea-State Related Altitude Errors in the SEASAT Radar Altimeter, *Journ. Geophys. Res.*, Vol. 87, No. C5, pp. 3227-3231, April 30, 1982.
- Kaula, W. M.; 1983, The Geopotential Research Mission, NASA HQ, Geodynamics Program, Washington, D.C.

- Koshlyakov, M. N., & Monin, A. S.; 1978, Synoptic Eddies in the Ocean, Ann. Rev. Earth Planet. Sci., Vol. 6, pp. 495-523.
- Levitus, S., & Oort, A. H.; 1977, Global Analysis of Oceanographic Data, Bull. Am. Meteorol. Soc., Vol. 58, No. 12, pp. 1270-1284, December 1977.
- Lorell, J., Colquitt, E., & Anderle, R. J.; 1982, Ionospheric Correction for SEASAT Altimeter Height Measurement, Journ. Geophys. Res., Vol. 87, No. C5, pp. 3207-3212, April 30, 1982.
- Lorell, J., Parke, M. E., & Scott, J. F.; 1980, Seasat Geophysical Data Record (GDR) Users Handbook, Altimeter. Report 622-97, Revision A, Jet Propulsion Laboratory, Pasadena, CA, 66 pp., September 15, 1980.
- Molodensky, M. S., Eremeev, V. F., and Yurkina, M. I., 1962, Methods for Studying the External Gravitational Field and Figure of the Earth, Israel Program for Scientific Translations, 248 pp.
- Moritz, H., 1974, Some First Accuracy Estimates for Applications of Aerial Gradiometry, Rept. Dept. Geod. Sci. No. 209, The Ohio State University, Columbus, OH, 72 pp.
- Parke, M. E.; 1980, Detection of Tides from the Patagonian Shelf by the Seasat Radar Altimeter: An Initial Comparison, Deep Sea Res., 27A, pp. 297-300.
- Parke, M. E., & Henderschott, M. C.; 1980, M2, S2, K1 Models of the Global Ocean Tide on an Elastic Earth, Marine Geod., Vol. 3, pp. 479-508.
- Rapp, R. H.; 1982, A Summary of the Results from the OSU Analysis of Seasat Altimeter Data, Report No. 335, Department of Geodetic Science, The Ohio State University, Columbus, OH 43210, pp. 19, August 1982.
- Schwiderski, E. W.; 1980a, Global Ocean Tides 1: A Detailed Hydrodynamical Interpolation Model, Marine Geod., Vol. 3, pp. 161-217.
- _____, 1980b, Ocean Tides 2: A Hydrodynamical Interpolation Model, Marine Geod., Vol. 3, pp. 219-255.
- _____, 1980c, On Charting Global Ocean Tides, Rev. Geophys. Space Phy., Vol. 18, No. 1, pp. 243-268.
- Tai, C., & Wunsch, C.; 1983, Absolute measurement by satellite altimetry of dynamic topography of the Pacific Ocean, Nature, Vol. 301, pp. 408-410, February 1983.

- Tapley, B. D., Born, G. H., & Parke, M. E.; 1982, The SEASAT Altimeter Data and its Accuracy Assessment, Journ. Geophys. Res., Vol. 87, No. C5, pp. 3179-3188, April 30, 1982.
- Tapley, B. D., Lundberg, J. B., & Born, G. H.; 1982, The SEASAT Altimeter Wet Tropospheric Range Correction, Journ. Geophys. Res., Vol. 87, No. C5, pp. 3213-3220, April 30, 1982.
- West, G. B.; 1981, Seasat Satellite Radar Altimetry Data Processing System, NSWC TR 81-234, Naval Surface Weapons Center, Dahlgren, VA 22448, 28 pp., May 1981.
- Wisler, M. M., & Hollinger, J. P.; 1977, Estimation of marine environmental parameters using microwave radiometric remote sensing systems, NRL Memo. Rep 3661, Naval Res. Lab., Washington, D.C.
- Wunsch, C.; 1978, The North Atlantic Circulation West of 50 W Determined by Inverse Methods, Rev. Geophys. Space Phys., Vol. 16, No. 4, pp. 583-620, November 1978.
- _____ ; 1981a, Low-Frequency Variability of the Sea, in Evolution of Physical Oceanography, B. A. Warren and C. Wunsch eds., MIT Press, Cambridge, MA, pp. 342-374.
- _____ ; 1981b, Satellite Altimetric Measurements of the Ocean, Report of the TOPEX Science Working Group. Jet Propulsion Laboratory, Pasadena, CA, 78 pp., March 1, 1981.
- Wunsch, C., & Gaposchkin, E. M.; 1980, on using satellite altimetry to determine the general circulation of the oceans with applications to geoid improvement. Rev. Geophys. Space Phys., Vol. 18, pp. 725-745.
- Wyrтки, K.; 1974, The Dynamic Topography of the Pacific Ocean and its Fluctuations, Hawaii Institute of Geophysics, University of Hawaii, 61 pp., August 1974.
- _____ .; 1975, Fluctuations of the Dynamical Topography in the Pacific Ocean, Journ. Phys. Oceanogr., Vol. 5, pp. 450-459.

APPENDIX A

ERROR COEFFICIENTS R_n

\

TABLE I(a) R_n coefficients for $\psi_0 = 5$ to 180 degrees
n = 0 to 10

ψ_0	R ₀	R ₁	R ₂	R ₃	R ₄	R ₅	R ₆	R ₇	R ₈	R ₉	R ₁₀
5	87.70234	80.05160	72.74854	65.79276	59.18195	52.91350	46.98414	41.38936	36.12646	31.18854	26.57052
10	41.89485	34.59210	27.98129	22.05193	16.78843	12.17041	8.17296	4.76704	1.91990	-.40447	-2.24474
15	26.64519	19.68940	13.76003	8.82210	4.82465	1.70242	-.62196	-2.23540	-3.23160	-3.70808	-3.76321
20	19.03508	12.42427	7.16075	3.16328	.31609	-1.52422	-2.52045	-2.84562	-2.67363	-2.17038	-1.48597
25	14.48091	8.21242	3.59434	.47203	-1.36834	-2.18045	-2.23568	-1.80049	-1.11612	-.38230	.25328
30	11.45481	5.52537	1.52777	-.79679	-1.79321	-1.84854	-1.34545	-.62016	.06881	.57524	.77582
35	9.30204	3.70768	-.30145	-1.31238	-1.63794	-1.20303	-.47787	.18637	.58811	.67209	.49730
40	7.69522	2.43138	-.41637	-1.41328	-1.24195	-.58803	.13073	.53245	.57379	.34641	.02133
45	6.45250	1.51397	-.81144	-1.28908	-.78681	-.05356	.43470	.51877	.29150	-.03320	-.25710
50	5.46481	.84575	-.99621	-1.05310	-.36998	.26505	.48370	.30926	-.01555	-.23939	-.24763
55	4.66272	.35671	-1.04291	-.77550	-.03947	.40605	.36731	.05811	-.20053	-.23052	-.07295
60	4.00000	-.00000	-1.00000	-.50000	.18750	.40625	.17969	-.12891	-.22583	-.09167	-.90773
65	3.44464	-.25697	-.90108	-.25304	.31323	.31426	-.00214	-.20636	-.13515	.05528	.13857
70	2.97379	-.43760	-.76999	-.04929	.35188	.17881	-.12909	-.18133	-.11720	.12552	.07571
75	2.57072	-.55919	-.62382	.10491	.32398	.04105	-.18196	-.09373	.08795	.10244	-.12204
80	2.22290	-.63480	-.47488	.20906	.25322	-.06976	-.16668	.00662	.11543	.02544	-.07810
85	1.92075	-.67453	-.33192	.26674	.13883	-.13772	-.10565	.07923	.08036	-.04707	-.06493
90	1.65685	-.68629	-.20101	.28427	.06245	-.15938	-.02765	.10408	.01483	-.07441	-.00897
95	1.42537	-.67641	-.08612	.26955	-.02224	-.14118	.04101	.08319	-.04301	-.05141	-.04060
100	1.22163	-.65002	.01043	.23118	-.08565	-.09591	.08276	.03470	-.06747	-.00282	-.05046
105	1.04189	-.61128	.08762	.17776	-.12318	-.03890	.09136	-.01719	-.05405	.03738	.02217
110	.88310	-.56369	.14547	.11726	-.13470	.01543	.07114	-.05216	-.01696	.04723	-.01639
115	.74276	-.51011	.18485	.05663	-.12368	.05610	.03365	-.06026	.02130	.02691	-.03575
120	.61880	-.45299	.20726	.00149	-.09603	.07708	-.04353	-.04205	.04205	-.00578	-.02575
125	.50953	-.39439	.21467	-.04408	-.05888	.07755	-.03810	-.01296	.03850	-.02907	.00100
130	.41351	-.33603	.20941	-.07754	-.01943	.06112	-.05250	.01719	.01676	-.03075	.02227
135	.32957	-.27939	.19403	-.09790	.01605	.03434	-.04884	.03539	-.00933	-.01368	.02371
140	.25671	-.22575	.17118	-.10554	.04294	.00487	-.03144	.03673	-.02626	.00856	.00782
145	.19412	-.17615	.14350	-.10200	.05870	-.02037	-.00793	.02372	-.02739	.02169	-.01082
150	.14110	-.13149	.11356	-.08969	.06295	-.03658	.01352	.00408	-.01509	.01948	-.01825
155	.09712	-.09251	.08374	-.07161	.05724	-.04188	.02681	-.01322	.00200	.00625	-.01128
160	.06171	-.05983	.05620	-.05102	.04460	-.03732	.02959	-.02182	.01442	-.00774	.00205
165	.03452	-.03393	.03276	-.03107	.02891	-.02634	.02345	-.02035	.01711	-.01385	.01066
170	.01528	-.01516	.01493	-.01459	.01414	-.01360	.01296	-.01224	.01145	-.01060	.00970
175	.00381	-.00380	.00379	-.00377	.00374	-.00370	.00366	-.00361	.00356	-.00349	.00343
180	0.00000	0.00000	0.00000	0.00000	0.00000	0.00000	0.00000	.00000	.00000	.00000	.00000

FILM
4-8